International Journal of Thermophysics, Vol. 28, No. 1, February 2007 (© 2007)
DOI: 10.1007/s10765-007-0163-5

Thermal Diffusivity Measurements of CMSX-4 Alloy by the Laser-Flash Method

R. Abdul Abas,[1] M. Hayashi,[1] and S. Seetharaman,[1,2]

Received: November 4, 2005

In the present work, thermal diffusivity measurements have been carried out on industrial samples of CMSX-4 nickel-base superalloy using the laser-flash method with emphasis on studying the effect of temperature and microstructure on the thermal diffusivity. The measurements were performed in the temperature range from 298 to 1623 K covering both solid as well as liquid ranges. Below 1253 K, the thermal-diffusivity values were found to increase with increasing temperature. Microstructural investigations of quenched samples revealed that below 1253 K, an ordered phase, usually referred to as the γ'-phase was present together with the disordered fcc phase, often referred to as the γ phase. Between 1253 K and the solidus temperature, the γ' phase was found to dissolve in the matrix alloy causing an increase in the disordering of the alloy, and thereby a small decrease in the thermal-diffusivity values. The thermal-diffusivity values of samples pre-annealed at 1573 K exhibited constancy in the temperature range from 1277 to 1513 K, which is attributed to the attainment of thermodynamic equilibrium. These equilibrium values were found to be lower than the results for samples not subjected to annealing. The thermal-diffusivity values of the alloy in the liquid state were found to be independent of temperature.

KEY WORDS: laser-flash method; phonon conduction; thermal conductivity; thermal diffusivity; γ and γ' phases.

1. INTRODUCTION

Thermophysical properties, such as thermal diffusivity and heat capacity, have both theoretical as well as practical importance. In many engineering

[1] School of Industrial Engineering and Management, Department of Materials Science and Engineering, Royal Institute of Technology, SE-100 44 Stockholm, Sweden.
[2] To whom correspondence should be addressed. E-mail: raman@kth.se

situations, it is necessary to have heat transfer data in order to calculate the ability of a structural component to conduct heat or to dissipate a large quantity of locally generated heat [1]. Thermal conductivities are also of fundamental interest as the mechanism of heat conduction is a structure-related phenomenon.

In recent years, mathematical modeling of the heat and mass transfer has proved to be a valuable tool in high-temperature process control such as steelmaking and designing heat-resistant materials such as Ni-base and Ti-base alloys. Thermophysical property data such as density, viscosity, surface tension, enthalpy, heat capacity, thermal conductivity, and thermal diffusivity are required for fluid-flow and heat-transfer computations in various processes [2]. The aim of the present study is to measure the thermal diffusivities of CMSX-4 alloy in both solid and liquid states from room temperature to 1620 K using a laser-flash technique. This work has been performed as part of the ESA (European Space Agency) project, "THERMOLAB" for precision measurement of thermophysical properties of industrial alloys with a goal to optimize industrial process design and product quality.

The methods for measuring the thermal diffusivity can be classified into two main groups: *viz*. periodic and nonperiodic heat-flow methods. The periodic methods include the Ångström, thermoelectric, and radial wave methods, while nonperiodic methods includes the bar, small area, semi-infinite plate, radial heat flow high-intensity arc, electrically-heated rod, and flash methods [3]. Most of these methods have inherent limitations due primarily to heat transport via convection as well as heat losses by radiation. The impact of these factors is minimized by the use of the laser-flash technique due to the small thickness of the sample and the high-speed heat supply to the specimen [4].

2. EXPERIMENTAL

2.1. Material

CMSX-4 nickel-base superalloy, used in the present work, was supplied by Doncasters Precision Castings Bochum GmbH, Germany. The chemical composition of the sample is given in Table I [5]. A high-purity argon gas (99.9999%, AGA, Sweden) atmosphere was used to prevent oxidation of the sample during measurements. In order to minimize impurity levels in the argon gas, it was subjected to a number of purification steps. The moisture impurity in the argon gas was removed by passing the gas successively through silica gel as well as $Mg(ClO_4)_2$. To remove traces of CO_2 in the gas, a column of ascarite was introduced in the system. The

Table I. Chemical Compositions (in mass%, except for O and S which are in ppm) of CMSX-4 Samples

Al	C	Co	Cr	Fe	Mo	Ni	O	Re	S	Si	Ta	Ti	W
5.6	.004		6.4	0.04	0.61		2[a]	2.9	2[a]	0.4	6.5	1.05	6.4
(6.7)		(9.7)	(6.4)	(0.1)	(0.6)	60.5		(2.9)			(6.5)	(1.0)	(6.4)

(Numbers in parentheses indicate the composition of sample used in preliminary experiments [5].)
[a]Indicates ppm.

gas was passed through columns of copper and magnesium turnings kept at 923 and 723 K, respectively. A titanium foil was placed beside the sample as an *in situ* oxygen getter. By using a ZrO_2–CaO oxygen sensor, the oxygen partial pressure in the argon cleaned in this way was found to be less than 10^{-17} Pa [6].

2.2. Thermal-Diffusivity Measurements

A Sinku-Riko laser-flash unit (Model TC-7000H/MELT), with a maximum sample temperature limit of 1873 K, was used for the present thermal-diffusivity measurements [7]. The furnace heating elements, eight in number, are made of lanthanum chromate and controlled by a PID controller within ±5 K at 1473 K. A sapphire crucible, which is transparent to laser beam and infrared radiation, was used as the sample holder. The sample temperature was measured using a Pt-13%Rh/Pt (R-type) thermocouple positioned in an alumina tube and placed close to the sample holder. The Nd-glass laser rod (10 mm in diameter, xenon exciting tube, 2.4 kV incident energy, and 6943 Å wavelength) was used in this method as a heat source. The top side of the disc of the material (10 mm diameter and 2 mm thickness) was irradiated with the laser beam, the latter providing an instantaneous energy pulse. The laser energy was absorbed at the top surface of the sample and was conducted through the sample. The temperature rise at the back surface of the sample was monitored with an infrared detector and the temperature rise was plotted against time. Figure 1 shows the relationship between two factors, V and W. Here, V is the ratio of the actual temperature to the maximum temperature $T/T_{\max}$ that can be used to represent the temperature rise of the rear face of the specimen, and W is given by the following equation: $W = \pi^2 \alpha t_{1/2}/L^2$, where α is the thermal-diffusivity of the sample ($cm^2 \cdot s^{-1}$) and L is the thickness of the sample. The temperature rise of the back surface is generally about 2 K. The value of V can vary between 0 and 1. The time at

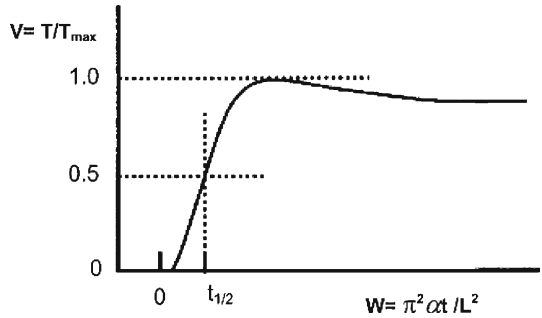

Fig. 1. Typical heat profile of the back surface of the sample during laser-flash measurement.

$V = 0.5$ is the half rise time $t_{1/2}$, i.e., the time required for the rear surface to reach half of the maximum temperature rise. Depending on the specimen and the thermal-diffusivity value, $t_{1/2}$ can range from a few ms to a few s. W is determined to be 1.37 by calibration experiments and was found to be independent of temperature within experimental uncertainties. Hence,

$$\alpha = 1.37L^2/\pi^2 t_{1/2}[8] \tag{1}$$

The calibration of the experimental apparatus was repeated between different measurements by carrying out room-temperature thermal-diffusivity measurements of solid stainless steel (SUS 304), which gave a thermal-diffusivity value of 3.81×10^{-6} $m^2 \cdot s^{-1}$ ($\pm 0.25\%$) at 295 K. This was found to be in accordance with recommended thermal-diffusivity values in the literature [9]. Furthermore, the calibration of the experimental apparatus for measurements with liquid samples was carried out by measuring the thermal diffusivity of liquid lead.

In the present study, the sample was prepared by polishing the surfaces. The parallelism of the surfaces was ensured by measuring the sample thickness at a number of places. In general, the sample was heated to 1573 K and cooled to room temperature at the rate of $6\,K \cdot min^{-1}$. Thermal-diffusivity measurements were carried out during three (heating–cooling) cycles mentioned above and one heating cycle. At each temperature, the sample was kept for at least 20 min in order to ensure that the sample had attained thermal equilibrium. The measurements were carried out by repeating the laser shots at least five times and ascertaining that the values were reproducible. Some selected experiments were repeated with different sample thicknesses in order to verify that the results were independent of

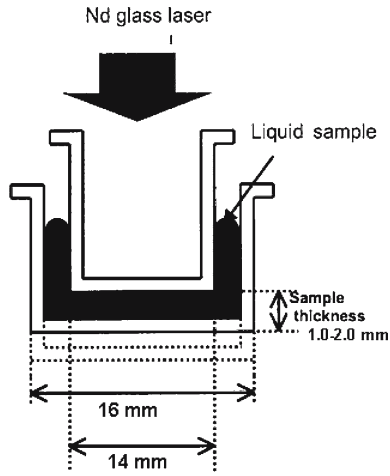

Fig. 2. Sample arrangement during liquid-state measurement using sapphire crucibles.

sample thickness. In view of the fact that the thermal history of the sample received was not defined, one sample was heated to 1573 K, kept for 12 h (which was found to be sufficient to bring the sample to thermodynamic equilibrium by microscopic studies of quenched samples carried out in the present laboratory) and brought down to lower temperatures for measurement under isothermal conditions. These measurements were carried out at 1531, 1403, and 1277 K in order to study the thermal diffusivity values under near-thermodynamic equilibrium conditions.

In the liquid state, the sample was sandwiched between two sapphire crucibles in order to obtain an accurate thickness of the sample. Figure 2 shows the sample arrangement during liquid-state measurements. The thickness was accurately measured by a micrometer screw gauge. The measurements were carried out for two different sample thicknesses similar to the method adopted by Waseda et al. [10].

In all cases, the samples were subjected to ocular and microscopic examinations after the experiments. No evidence of oxidation of the samples was detected.

2.3. Structural Studies

Four different heat-treatment sequences were adopted before carrying out the microscopic studies. The heat-treatment sequences of samples

Table II. Heat-Treatment Sequences of Samples A–E for Microstructure Studies

Sample	Annealing Temperature (K)	Water quenched temperature (K)	Note
A	600	600	–
B	1000	1000	–
C	1573	600	–
D	1573	1000	–
E	1373	1373	30 min annealing

A-D are given in Table II. Samples A and B were heated to 600 and 1000 K, respectively, at the rate of $6\,K \cdot min^{-1}$ and subsequently quenched into water. Samples C and D were heated to 1573 K at first, then cooled to 600 and 1000 K, respectively, at the rate of $6\,K \cdot min^{-1}$, and then quenched into water. These studies were designed so as to observe the microstructure changes in the alloy during different heat-treatment procedures and to correlate them, if possible, with the thermal diffusivities observed. These four samples and the as-delivered material were analyzed using a scanning electron microscope (SEM) and electron dispersion spectroscopy (EDS) attached to SEM. Thermal diffusivities of samples A–D were also carried out at room temperature.

3. RESULTS

In Fig. 3, all the experimental results of the thermal-diffusivity measurements with as-received alloy samples are presented as functions of temperature. The error bars in the figure indicate the scatter in the data obtained at the same temperature in one experiment with at least five different laser shots. In general, the scatter in the values was less at lower temperatures, and become more significant as the temperature was increased. The scatter can be represented by a standard deviation of around ±2–8%. This is attributed by the authors to the variations in the furnace temperature as well as, in some cases, to the sample still undergoing structural changes during measurements. The change of the position of the gold mirror could contribute to the scatter. Despite the precautions taken in sample preparation, slight deviations from the parallelism of the surfaces could cause error, and this is difficult to detect. The measurements at about 600 K showed unusually large scatter. The reason for this is uncertain.

It can be seen in Fig. 3 that the thermal-diffusivity increases with temperature up to 1223 K. Above this temperature, the diffusivity shows a slight decrease and/or become constant. In the solid–liquid zone, it is

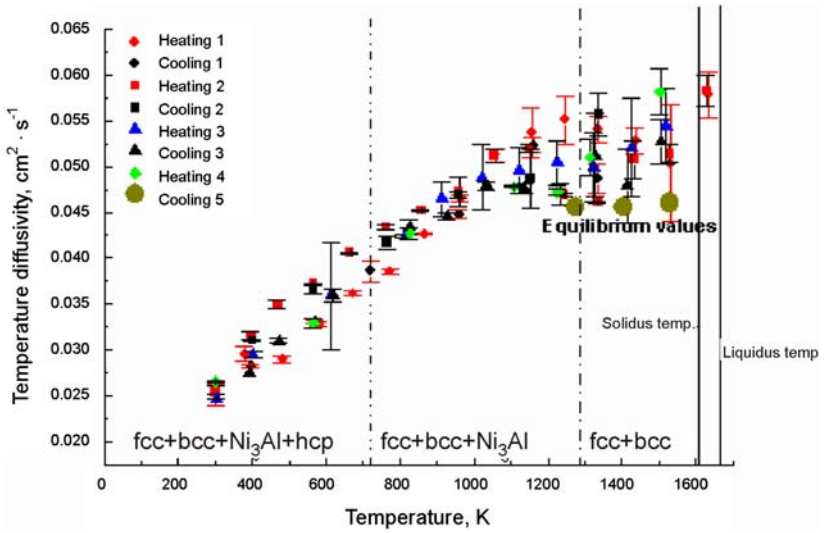

Fig. 3. Thermal-diffusivity temperature curves of CMSX-4 alloy.

difficult to observe any definite trend as the experimental scatter is significant. In fact, above 1223 K, different experimental runs give varying results, which could be due to the thermal history of the industrial sample received. It is also observed that the equilibrium values are less than the other values over the same temperature range.

Figure 4 shows SEM images of five different samples. Figures 4A and 4B correspond to samples A and B, heated to 600 and 1000 K, respectively, at the rate of $6\,\mathrm{K}\cdot\mathrm{min}^{-1}$ and subsequently quenched in water. Figure 4C and D correspond to samples C and D that were heated to 1573 K at first, then cooled to 600 and 1000 K, respectively, at the rate of $6\,\mathrm{K}\cdot\mathrm{min}^{-1}$, and then quenched in water. The figure also shows the microstructure of the as-received material. SEM images show the presence of the intermetallic γ' phase as well as the γ/γ' matrix. One sample was heat treated at 1373 K for 30 min and quenched in water. SEM examination of this sample (Fig. 4E) indicated that the amount of γ' precipitate decreased substantially. Table III shows the chemical analyses of these phases carried out using EDS attached to SEM. The thermal diffusivities of A–D at room temperature were 0.0266, 0.0213, 0.0232, and $0.0210\,\mathrm{cm}^2\cdot\mathrm{s}^{-1}$, respectively.

Figure 5 shows thermal-diffusivity measurements in the liquid state. The figure shows that the liquid thermal diffusivity does not show any significant change with temperature.

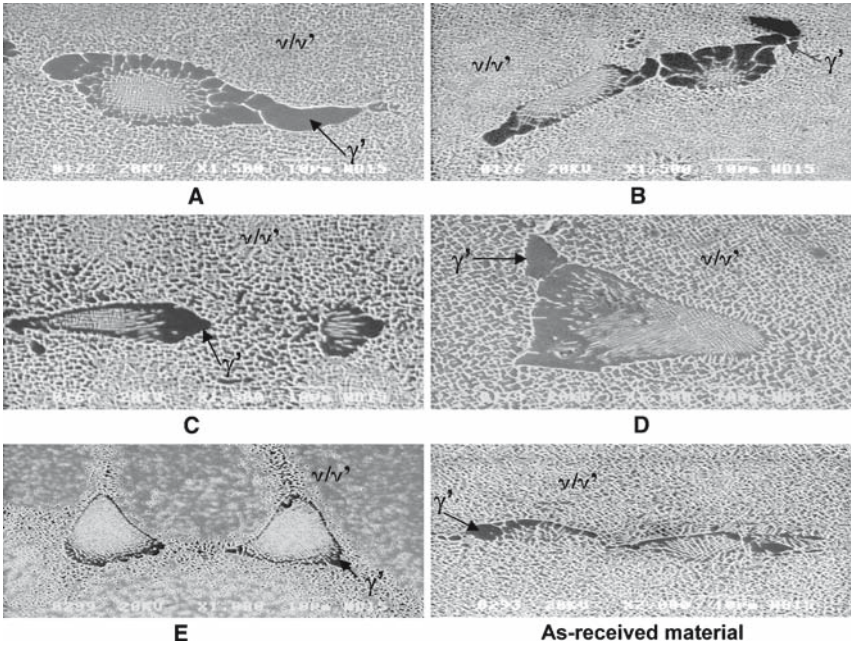

Fig. 4. SEM pictures of annealed CMSX-4 alloys: (A,B) quenched from 600, 1000 K; (C,D) quenched samples after heating to 1573 and cooling to 600 and 1000 K; and (E) annealed sample at 1373 K for 30 min and quenched in water and as-received material. Magnification = 1500X.

4. DISCUSSION

Figure 6 shows the phase diagram of an alloy close to that of the CMSX-4 nickel-base alloy used in the present work calculated by using Thermo-calc software. For the sake of simplicity, Ti (1.06 mass%) was not taken into account in these calculations. More detailed calculations carried out in the Division of Process Sciences, Royal Institute of Technology show that the phase distribution is essentially the same as presented in Fig. 6. It can be seen that the material contains fcc + bcc + hcp + Ni_3Al (γ'phase) at temperatures below 1273 K. In the presence of Ti, corresponding Ti- could be expected to dissolve and form a solid solution. Above this temperature, only fcc + bcc phases are stable, and the γ'phase starts dissolving in significant amounts into the γ-phase. According to Fig. 6, the solidus temperature is 1609 K and the liquidus temperature is 1670 K.

Table III. Chemical Composition (in mass%) of Annealed CMSX-4 Samples A–E as Determined by EDS Attached to SEM

Structure	Ni	Co	Cr	Ti	Si	Al	Re
As delivered material							
γ/γ'	63.02	11.20	8.02	0.96	2.20	4.02	4.81
γ'	73.84	8.65	3.34	1.49	4.30	6.32	1.49
Sample A							
γ/γ'	66.02	11.23	7.69	1.1	2.47	4.47	1.03
γ'	74.00	9.05	3.22	1.73	3.8	6.54	0.87
Sample B							
γ/γ'	66.02	12.98	7.09	0.80	2.03	4.52	0.98
γ'	74.72	9.14	3.1	1.88	4.28	6.46	0.65
Sample C							
γ/γ'	66.82	11.38	8.05	0.89	2.32	4.38	1.05
γ'	77.07	8.96	2.99	1.63	3.66	6.16	0.96
Sample D							
γ/γ'	67.13	11.11	8.16	1.18	2.17	4.34	1.05
γ'	74.44	9.5	3.63	1.77	4.19	6.47	0.56
Sample E							
γ/γ'	61.61	10.98	7.22	0.74	1.62	4.30	6.06
γ'	73.94	8.57	3.36	1.68	4.23	6.67	1.02

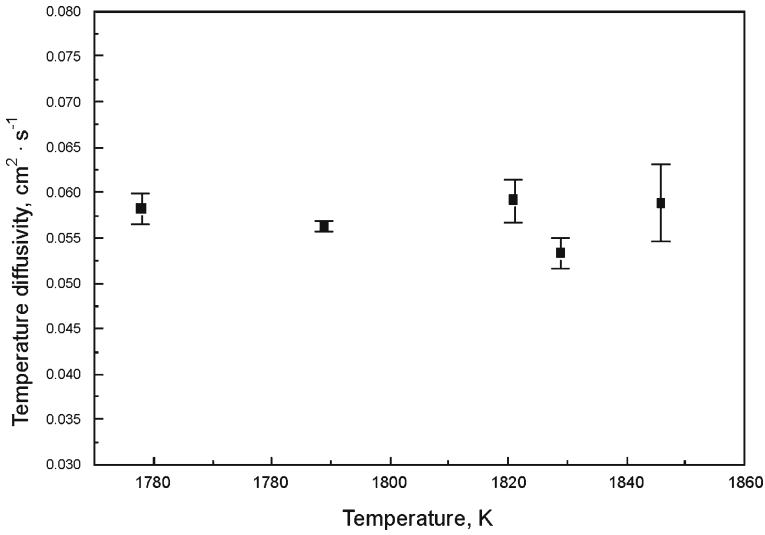

Fig. 5. Results of thermal-diffusivity measurements for liquid CMSX-4 alloy.

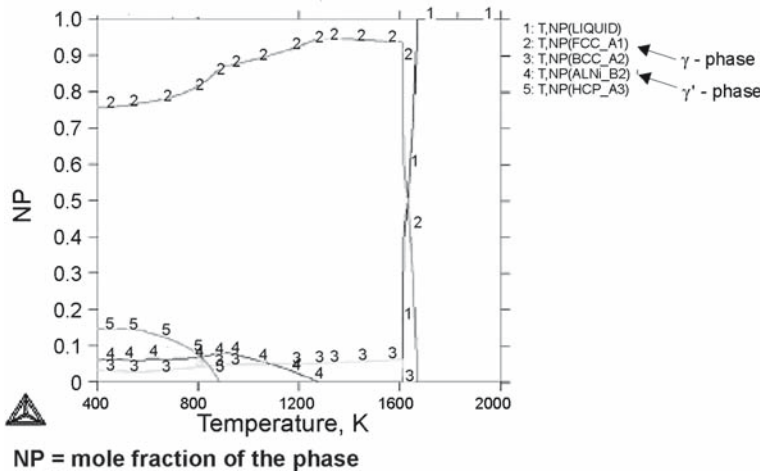

Fig. 6. Calculated phase diagram of an alloy with composition close to the present CMSX-4 alloy using Thermo-calc software.

The thermal conductivity of CMSX-4 alloy, investigated in the present work, could be calculated from the values of the specific heat and density according to the formula,

$$\kappa = \alpha C_p \rho \tag{2}$$

where κ is the thermal conductivity, α is the thermal diffusivity, C_p is the heat capacity, and ρ is the density.

The heat-capacity values of the CMSX-4 alloy investigated in the present work have been measured by Tonooka [11]. The results of these measurements are presented in Fig. 7. No information regarding the impact of structural changes of the alloy on the heat-capacity results had been presented by this author. Hence, the present authors do not attempt to relate the reported heat capacities to structural aspects. These results were used only to estimate the trend in the thermal conductivity of the CMSX-4 alloy investigated. The densities of the same alloy have been measured as part of the THERMOLAB project [12]. The results are presented in Table IV. The thermal conductivities calculated by combining the above data with the present results are presented in Fig. 8. For the above calculations, the average values of thermal diffusivities from Fig. 3 were used.

The thermal conductivity κ can be considered to be due to electron and phonon conduction. According to Debye [13], the thermal-diffusivity can be expressed by the equation,

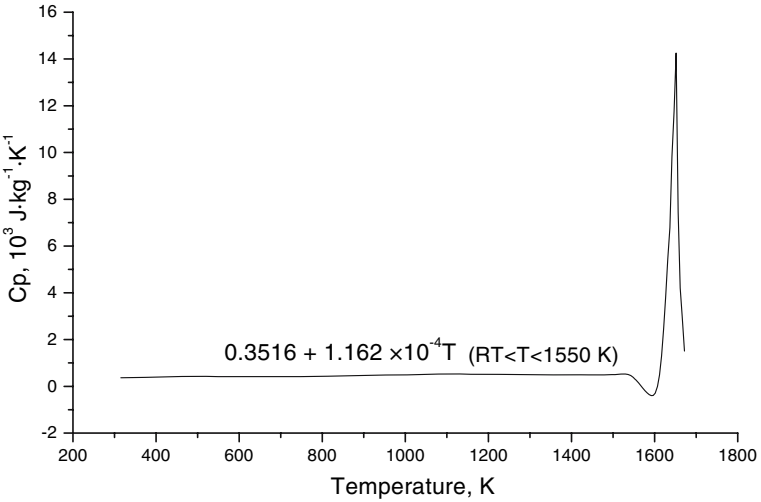

Fig. 7. Heat capacity of CMSX-4 alloys in the temperature range of 300 to 1700 K [7].

Table IV. Densities of CMSX-4 Alloy at Different Temperatures [10]

T (K)	298	473	673	873	1073	1173	1273	1373	1473	1593	1653
ρ ($\mathrm{kg \cdot m^{-3}}$)	8345	8308	8246	8177	8109	8075	8043	8017	7666	7898	7575

$$\kappa = \frac{1}{3} n C_{\mathrm{v}} v l \tag{3}$$

where n is the number of particles per unit volume, C_{V} is the heat capacity at constant volume per particle (so that nC_{v} is the heat capacity per unit volume expressed in $\mathrm{J \cdot m^{-3} \cdot K^{-1}}$), v is the speed of sound, and l is the mean free path [7,14]. Assuming that the speed of sound,v, is constant, the thermal conductivity will be proportional to the mean free path of electrons or phonons. The term l is dependent on collisions between electrons or phonons as well as on lattice defects.

The Wiedemann-Franz law [15] could be used to estimate the thermal conductivities from the electrical conductivities. This is represented as

$$\kappa / \sigma_{\mathrm{e}} T = 2.45 \times 10^{-8} W \cdot \Omega \cdot K^{-2} \tag{4}$$

where κ is the thermal conductivity in $\mathrm{W \cdot m^{-1} \cdot K^{-1}}$, σ_{e} is the electrical conductivity in $\Omega^{-1} \cdot \mathrm{m}^{-1}$, and T is the absolute temperature in K.

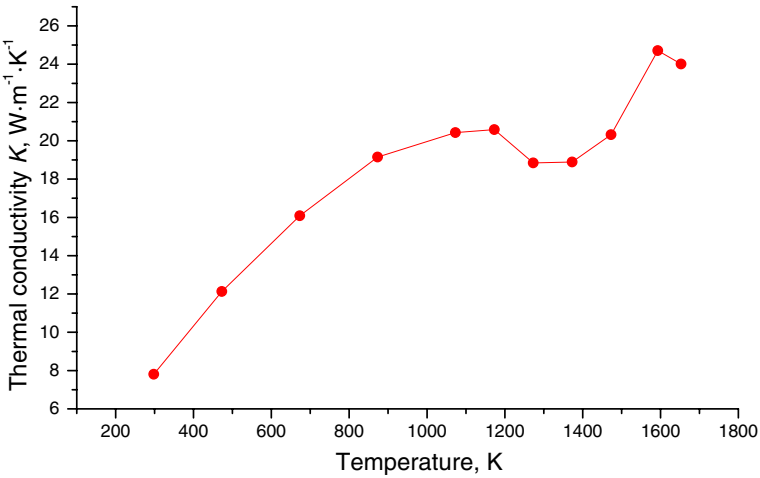

Fig. 8. Thermal-conductivity of CMSX-4 alloy as a function of temperature.

By using the Wiedemann-Franz law, the thermal conductivity of CMSX-4 alloy was calculated at room temperature to be 4.755 $W \cdot m^{-1} \cdot K^{-1}$, from the electrical-conductivity value of 65.13×10^4 $\Omega^{-1} \cdot m^{-1}$ [16]. At 1200 K, the thermal conductivity was 16.554 $W \cdot m^{-1} \cdot K^{-1}$, estimated from the electrical-conductivity value of 226.74×10^4 $\Omega^{-1} \cdot m^{-1}$ [16]. Experimental values show that the thermal conductivity values of this alloy are 7.807 and 20.584 $W \cdot m^{-1} \cdot K^{-1}$ at room temperature and 1200 K, respectively. Thus, it can be concluded that the heat is conducted in this alloy by phonons as well as electrons and the electron contribution increases from 60% at room temperature to 80% at 1200 K.

The situation in the present case is complicated due to the industrial sample being investigated, where the precipitation of the intermediate γ' phase might not have reached an equilibrium state. The as-received sample is shown to have a fine $\gamma - \gamma'$ structure as shown in Fig. 4. The γ' phase has an ordered structure. Thus, it is likely to have a higher electrical conductivity. As the sample is heated, the γ'-phase gets coarsened as is seen in Fig. 4. Thus, the increase of thermal conductivities below 1270 K may partly be attributed to the increase in the electronic contribution to conduction as indicated by electrical-conductivity values as well as due to the coarsening effect of the γ'-phase. The γ'-phase starts dissolving in the γ-phase above approximately 1270 K, which is evident in Fig. 4E. This would result in a decrease in the thermal conductivity as was found in the present experiments.

In the liquid state, the average value of the thermal diffusivities of the liquid alloy was $0.058\,cm^2 \cdot s^{-1}$, and it can be seen that there is no significant change with increasing temperature. It may be attributed to the mean free path being shorter than the characteristic distance between two neighboring atoms. It is recognized that the present thermal-diffusivity values in the liquid state could be affected by a certain degree of convection (the upper liquid surface was 2 K higher than the bottom, and thus the convective force has to work against gravity) as well as due to the free-liquid surface between the crucibles, which was about 12% of the total sample surface as shown in Fig. 2.

5. CONCLUSIONS

In the present work, thermal-diffusivity measurements have been performed on a CMSX-4 nickel-base superalloy to investigate the effect of temperature on the thermal diffusivity of this alloy. The measurements were carried out between room temperature and the liquidus temperature. Below 1253 K, the thermal diffusivity increases with temperature. This phenomenon is independent of microstructure. The intermediate Ni_3Al, Ti -γ' phase was found together with the γ-phase in this temperature range. Between 1253 K and the liquidus temperature, the thermal diffusivities show nearly-constant values. The thermal behavior of the samples is complicated due to the nature of the as-received industrial samples, where the system is away from thermodynamic equilibrium. The thermal diffusivities of samples annealed at 1573 K and measured at 1277, 1403, and 1531 K did not show any noticeable change in thermal diffusivities with time, indicating the attainment of equilibrium. These values were found to be lower than the thermal diffusivities of non-annealed samples. This is attributed to the dissolution of the γ' phase in the matrix. The thermal diffusivities measured in the liquid state did not show any significant change with temperature.

ACKNOWLEDGMENTS

The authors acknowledge the financial support received from the European Space Agency for the project "THERMOLAB" for carrying out the present investigation. The authors are also grateful to Dr. L. Teng for valuable discussions during the work.

REFERENCES

1. J. Ormerod, R. Taylor, and J. Edward, *Metal Technol.* 109 (1978).
2. K. C. Mills, A. P. Day, and P. N. Quested, *Int. J. Thermophys.* **18**:471 (1997).

3. R. E. Taylor, *High Temp.-High Press.* **11**:43 (1979).
4. J. T. Schirempf, *High Temp.-High Press.* **4**:411 (1972).
5. P. Quested, *Thermolab Mid-term Activity Report for the Period Sept. 1, 2001 – August 1, 2002* (National Physical Laboratory, Teddington, Middlesex, United Kingdom 2002).
6. L. Teng, X. G. Lu, R. Aune, and S. Seetharaman, *Metall. Mater. Trans.* **35A**:3673 (2004).
7. R. Eriksson, M. Hayashi, and S. Seetharaman, *Int. J. Thermophys*. **24**:785 (2003).
8. W. J. Parker, R. J. Jenkins, C. P. Butler, and G. L. Abbott, *J. Appl. Phys.* **32**:1697 (1961).
9. H. Bogaard, P. D. Desai, H. H. Li, and C. Y. Ho, *Thermochim. Acta* **218:**373 (1993).
10. Y. Waseda, M. Masuda, and H. Ohta, *Proc. 4th Int. Symp. Advanced Nuclear Energy Research* (Mito, Ibaraki, Japan), p. 301.
11. Y. Tonooka, *M. Sc. Thesis* (Division of Materials Process Science, Royal Institute of Technology, Stockholm, Sweden, 2005).
12. *THERMOLAB Project*, European Space Agency (2002).
13. P. Debye, *Vorträge über die kinetische Theorie der Materie und Elektrizität*, Gottinger Wolfskehlvortrage (B. G. Teubner, Leipzig and Berlin, 1914), p. 46.
14. G. Grimvall, *Thermophysical Properties of Materials* (Elsevier Science B.V., Amsterdam, 1999).
15. T. Iida and R. I. L. Guthrie, *The Physical Properties of Liquid Metals* (Oxford Univ. Press, 1993), pp. 226–251.
16. K. C. Mills, Y. M. Youssef, and Z. Li, *ISIJ Int*. **46**:50 (2006).